Geochemical Perspectives Letters

Zircon growth experiments reveal limited equilibrium Zr isotope fractionation in magmas

H.G.D. Tompkins[1], M. Ibañez-Mejia[1*], F.L.H. Tissot[2], E. Bloch[3], Y. Wang[1,4], D. Trail[4]

https://doi.org/10.7185/geochemlet.2310

Abstract

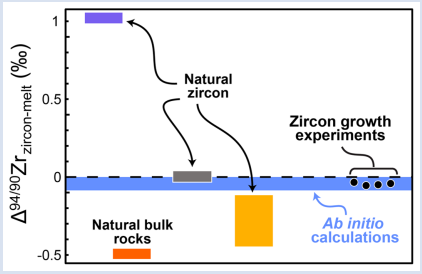

Recent studies of zirconium isotopes in igneous systems have revealed significant mass dependent variability, the origin of which remains intensely debated. While magmatic zircon crystallisation could potentially drive equilibrium isotope fractionation, given that Zr^{4+} undergoes a shift in coordination as zircon precipitates from a silicic melt, *ab initio* calculations predict only limited equilibrium fractionation between zircon and melt at magmatic temperatures. To resolve this debate, we determined the isotopic fractionation between co-existing zircon and silicic melt using controlled zircon growth experiments. Our experimental results indicate that zircon has a lower $\delta^{94/90}Zr$ relative to co-existing melt by ~0.045 ‰ at magmatic conditions, which is in excellent agreement with *ab initio* predictions. Our results imply that, for most natural systems studied to date, the observed variability is predominantly a result of non-equilibrium rather than equilibrium isotope fractionation during zircon crystallisation.

Received 27 October 2022 | Accepted 1 March 2023 | Published 28 March 2023

Introduction

Zirconium (Zr) belongs to a group of transition metals known as the high field strength elements, which due to their distinctive geochemical properties are used to trace magmatic differentiation and the co-evolution of Earth's mantle and crust. While studies of Zr stable isotope variation (expressed as $\delta^{94/90}Zr = [(^{94}Zr/^{90}Zr)_{Sample}/(^{94}Zr/^{90}Zr)_{Standard} - 1]\cdot1000$) have all linked Zr isotopic variability to zircon crystallisation during magmatic differentiation, they have also yielded conflicting observations regarding the direction and magnitude of Zr isotope fractionation in magmatic systems. Based on a $\delta^{94/90}Zr$ *vs.* SiO_2 trend in volcanic rocks from Hekla, Iceland, Inglis *et al.* (2019) suggested zircon is isotopically light compared to coexisting melt, and inferred a fractionation factor $\Delta^{94/90}Zr_{zircon\text{-}melt}$ (*i.e.* $\approx1000\cdot\ln(\alpha_{zircon\text{-}melt})$, where $\alpha_{zircon\text{-}melt} = [(^{94}Zr/^{90}Zr)_{Zircon}/(^{94}Zr/^{90}Zr)_{Melt}]$) of −0.5 ‰. Conversely, through measurement of single zircon and baddeleyite crystals from a gabbroic cumulate, Ibañez-Mejia and Tissot (2019) found these phases to be isotopically heavy relative to the starting melt using the bulk rock $\delta^{94/90}Zr$ as a proxy, and inferred a $\Delta^{94/90}Zr_{zircon\text{-}melt} = 1.06$ ‰. A subsequent study by Guo *et al.* (2020) observed internally zoned zircon with isotopically light cores and progressively heavier rims, which they interpreted as equilibrium Rayleigh fractionation of isotopically light zircon from a melt with $\Delta^{94/90}Zr_{zircon\text{-}melt}$ between −0.12 and −0.45 ‰. However, in all studies conducted to date on natural samples, no co-existing zircon-glass pairs have been directly measured. Rather, zircon-melt fractionation factors have only been inferred by calculation (*e.g.*, Rayleigh fitting or mass balance considerations).

Adding to this conundrum, no resolvable $\delta^{94/90}Zr$ variations (and therefore negligible fractionation) have been observed in several reference zircons (*e.g.*, 91500, Mud Tank, and Plešovice; Tompkins *et al.*, 2020; Zhang *et al.*, 2019), and recent *ab initio* calculations by Chen *et al.* (2020) and Méheut *et al.* (2021) predict that the magnitude of equilibrium Zr isotope fractionation at magmatic temperatures is too small ($\Delta^{94/90}Zr_{zircon\text{-}melt} \leq 0.08$ ‰) to explain the large fractionations observed in natural systems. Instead, both theoretical studies concluded that a combination of equilibrium and kinetic fractionation processes during crystallisation of zircon and rock forming minerals is necessary to produce the large variations observed in natural igneous systems.

Here, we address these conflicting observations from an experimental standpoint. Using zircon growth experiments performed under controlled laboratory conditions, we sought to determine the isotopic fractionation factor between zircon and melt ($\Delta^{94/90}Zr_{zircon\text{-}melt}$; hereafter $\Delta^{94/90}Zr$ for brevity) at various temperatures and melt compositions. To do so, experimental zircon and co-existing melts (quenched to a glass) were: 1) chemically separated using a novel sequential acid leaching procedure, and 2) their $\delta^{94/90}Zr$ were measured at high accuracy and precision using a ^{91}Zr-^{96}Zr double spike method.

1. Department of Geosciences, The University of Arizona, Tucson, AZ 85721, United States
2. The Isotoparium, Division of Geological and Planetary Sciences, California Institute of Technology, Pasadena, CA 91125, United States
3. School of Geosciences and the Environment, University of Lausanne, Lausanne, Switzerland
4. Department of Earth and Environmental Sciences, University of Rochester, Rochester, NY 14627, United States
* Corresponding author (email: ibanezm@arizona.edu)

Experimental Procedure and Samples

We utilised run products from zircon growth experiments performed by Wang and Trail (2019) and analysed: i) 11 experimental products published in Wang and Trail (2019), ii) three 'low temperature' (925 °C) experiments also performed by Wang and Trail (2019) but previously unpublished because they produced zircon crystals too small for that study, and iii) homogenised fractions of four starting base mixes that represent the starting composition (*i.e.* bulk system) for all experiments. Zircon growth experiments were performed in a piston cylinder apparatus at various temperatures and melt compositions (Table S-1). Various synthetic mixtures (dubbed 'base mixes') were prepared to simulate a range of hydrous felsic melts in the SiO_2-Al_2O_3-Na_2O-K_2O-CaO-ZrO_2-H_2O system with H_2O fixed at ~10 wt. % and doped with 500 ppm rubidium (Rb). Because Rb is highly incompatible in zircon, this trace element served as monitor for melt incorporation in the laser ablation study of Wang and Trail (2019), and was used as proxy for zircon-melt chemical separation in this study (see Supplementary Information). The base mixes covered a range of aluminum saturation indices (ASI = molar ratio of $Al_2O_3/[CaO + Na_2O + K_2O]$) alkalinity indices (A/NK = molar ratio of $Al_2O_3/[Na_2O + K_2O]$) and M factors (M = molar ratio of $[K + Na + 2Ca]/[Si \times Al]$), as these are useful criteria for characterising felsic rocks and parameterising zircon saturation in silicate melts (*e.g.*, Boehnke *et al.*, 2013). Further details about the experiments and run products can be found in Wang and Trail (2019).

The experiments studied here cover a wide range of temperatures (1400 °C to 925 °C), ASI (0.9 to 1.3), A/NK (1.4 to 2.2) and M parameters (1.2 to 1.8) (Table S-1). In all cases, the experimental products consisted of a mixture of glass (quenched melt) and zircon. Since the zircon crystals in all experiments are too small (mostly ≤20 μm in diameter) to physically separate from the glass, we designed an extraction procedure using sequential acid leaching to attain full chemical separation of these phases. Our calibrated protocol resulted in complete separation of glass from zircon, enabling each fraction to be independently spiked and prepared for isotopic analysis. Once separation was achieved, all fractions were measured for their $\delta^{94/90}$Zr relative to the NIST standard using the analytical methods described in Tompkins *et al.* (2020). Analytical methods are summarised in the Supplementary Information.

For each experimental product, we determined the total mass fraction of Zr removed from the liquid in the form of zircon relative to the bulk initial (*i.e.* *f* factor). Mean *f* values and their variability within the liquid at the time of quenching were determined *in situ* using Zr concentration measurements in glass fragments *via* secondary ion mass spectrometry (SIMS). The mean and variability in *f* values assigned in this manner were used to propagate uncertainties through all subsequent calculations. To ensure consistency, the mean *f* values determined using SIMS measurements of glass were verified using Zr/Rb measurements from solutions produced after acid leaching of glasses during preparation for isotopic analyses. Details about methods and calculations are included in the Supplementary Information.

Results

Results from all our measurements are reported in Tables S-2, S-3, and shown graphically in Figure 1. Experiments were found to yield mean *f* values between 0.12 ± 0.06 and 0.97 ± 0.01. The $\delta^{94/90}$Zr of the four base mixes were undistinguishable within uncertainty, and their mean value (0.054 ± 0.005 ‰) is depicted in Figure 1a (horizontal grey band). Results for all 14 zircon-glass pairs analysed are shown ranked by increasing mean *f*. All zircon fractions exhibit lower $\delta^{94/90}$Zr with respect to the bulk system, ranging from −0.168 ± 0.011 ‰ to −0.068 ± 0.013 ‰. In contrast, glasses have a bimodal $\delta^{94/90}$Zr distribution; six high temperature (1300 – 1400 °C) experiments yielded mean $f \leq 0.53$ and glass $\delta^{94/90}$Zr values indistinguishable from the bulk system within uncertainty (−0.057 ± 0.016 ‰ to −0.050 ± 0.013 ‰), while the eight experiments conducted at lower temperatures (925 – 1150 °C) yielded mean $f \geq 0.78$ and positive glass $\delta^{94/90}$Zr values (−0.004 ± 0.013 ‰ to +0.123 ± 0.013 ‰) compared to the bulk. Isotopic mixing calculations performed using the $\delta^{94/90}$Zr and *f* determined for each glass-zircon pair show excellent agreement within uncertainty with respect to the $\delta^{94/90}$Zr value of the starting base mix, thus confirming mass balance (Fig. 1b).

Discussion

The diffusivity of Zr^{4+} in zircon is expected to be extremely low even at magmatic temperatures (Cherniak *et al.*, 1997; Ibañez-Mejia and Tissot, 2019). Therefore, the growth of zircon from a magma removes Zr as a Rayleigh-type process even if chemical and isotopic equilibrium partitioning between the solid and melt are maintained, where only the outermost rim of the crystal is in equilibrium with the immediately surrounding melt while interior domains of the zircon become isolated from the rest of the system (Criss, 1999). In an equilibrium Rayleigh scenario, one could directly recover $\Delta^{94/90}$Zr from experiments by measuring the isotopic composition of the outermost zircon rim and melt in direct equilibrium, but this is impossible to achieve using our experimental setup. Instead, our chemical separation method produces bulk glass and bulk (*i.e.* cumulative) zircon fractions, meaning that we can only capture the total integrated isotopic effects that a Rayleigh-type process imposes on $\delta^{94/90}$Zr over the entire *f* interval of the experiment.

To approximate $\Delta^{94/90}$Zr using the results of Figure 1a, we took an inverse approach that treats each zircon crystallisation experiment as an equilibrium Rayleigh fractionation. The recovered $\Delta^{94/90}$Zr are summarised in Figure 1c, where they are compared with theoretically predicted values at 1300 – 700 °C from *ab initio* calculations. While all but one of our experiments conform to mass balance (Fig. 1b), for most high T experiments (low *f*) the $\delta^{94/90}$Zr of the zircon, glass, and bulk system could not all be exactly fitted using an equilibrium Rayleigh fractionation inversion. For experiments where $f \leq 0.53$, zircon fractions have $\delta^{94/90}$Zr values that are 'too low' for their respective mean *f* if an *equilibrium* process is assumed. For these experiments, we used the absolute difference in $\delta^{94/90}$Zr between the glass and bulk zircon measurements (a parameter we refer to as $\Delta^{94/90}Zr_{apparent}$), as a *maximum* permissible limit for the $\Delta^{94/90}$Zr governing that experiment (see Supplementary Information for a detailed rationale of this approach).

In general, all of the $\Delta^{94/90}Zr_{apparent}$ values determined from high T (low *f*) experiments, as well as the best fit $\Delta^{94/90}$Zr values from Rayleigh inversion of low T (high *f*) experiments, indicate that: i) zircon is invariably isotopically light relative to the melt from which it precipitates, and ii) that the magnitude of the fractionation factor between zircon and melt ($\Delta^{94/90}$Zr) is always smaller than −0.139 ‰ over the experimental temperature range. Details of the mathematical approach and parameters used to estimate $\Delta^{94/90}$Zr and calculate uncertainties are included in the Supplementary Information.

To explore whether temperature and/or melt compositional differences are controlling the variable fractionations observed between experiments, Figure 2 shows the fractionation

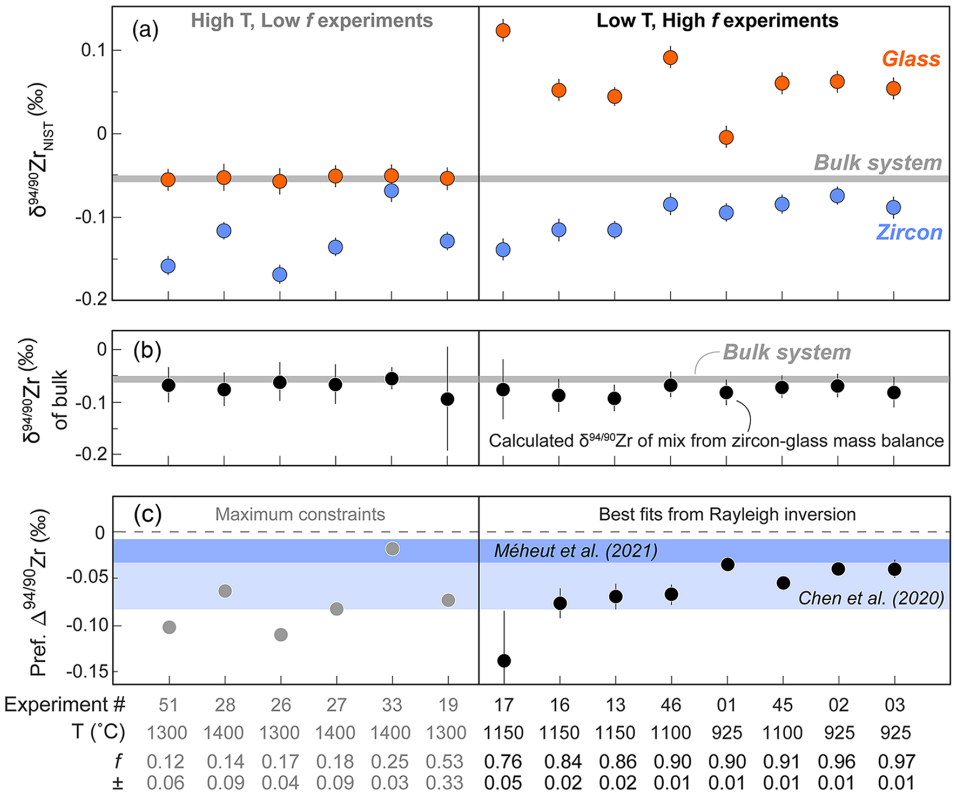

Figure 1 **(a)** $\delta^{94/90}$Zr of the glass (orange) and bulk zircon (blue) for each experiment. 'Bulk system' is the mean value of all experimental base mixes. **(b)** Mass balance calculations for all glass-zircon pairs compared to the $\delta^{94/90}$Zr of the bulk starting mix. **(c)** Apparent $\Delta^{94/90}$Zr, the fractionation factor between zircon and melt, determined for each experiment (see text for further details and discussion). Range of *ab initio* values between 1300 °C and 700 °C (Chen *et al.*, 2020; Méheut *et al.*, 2021) are shown as horizontal blue bands. Samples are shown rank ordered by increasing mean *f*. Uncertainties, visible only when larger than the symbols, are 2σ.

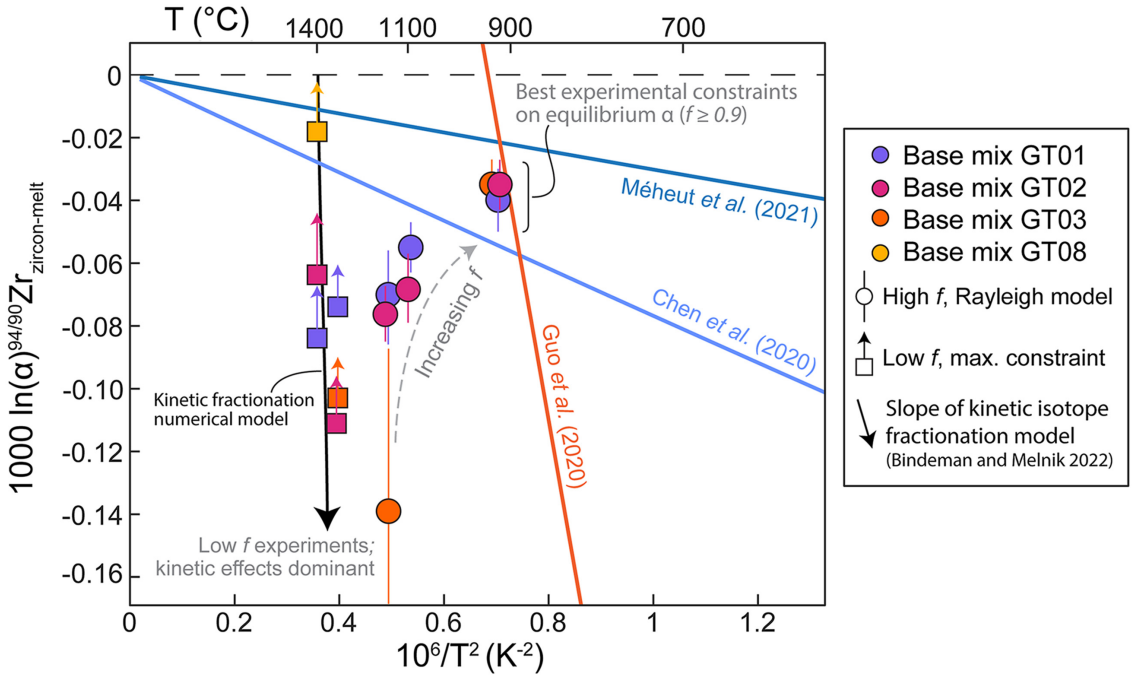

Figure 2 Temperature dependence of zircon-melt fractionation factors from *ab initio* studies (Chen *et al.*, 2020; Méheut *et al.*, 2021), natural samples (Guo *et al.*, 2020), and our experiments. Circles are low T, high *f* experiments in Figure 1, from which $\Delta^{94/90}$Zr was retrieved using Rayleigh inversion. Squares denote high T, low *f* experiments, where only a *maximum* magnitude for fractionation ($\Delta^{94/90}Zr_{apparent}$) in that experiment could be constrained (see text). Black solid line is the slope of kinetic isotope fractionation during diffusion limited growth of a zircon nucleating at 1400 °C, calculated using the numerical code of Bindeman and Melnik (2022) (see Supplementary Information for details).

results of Figure 1c plotted as a function of their inverse squared temperature. The *ab initio* zircon fractionation models of Chen *et al.* (2020) (relative to Ca-catapleiite) and Meheut *et al.* (2021) (relative to gittinsite) are shown for comparison, as well as the model of Guo *et al.* (2020), obtained from Rayleigh inversion of $\delta^{94/90}$Zr zoning in natural zircon. It is important to note, however, that because the Guo *et al.* (2020) model does not result in a $\Delta^{94/90}Zr = 0$ at infinite temperature (*i.e.* $1/T^2 = 0$), it has little physical meaning and, unlike as argued in that study, cannot represent an equilibrium fractionation process (Schauble *et al.*, 2009; Young *et al.*, 2015).

Close inspection of Figure 2 reveals that our data do not plot along a single slope in $\Delta^{94/90}$Zr *vs.* $1/T^2$ space, which clearly indicates that effects other than equilibrium isotope partitioning are influencing the $\Delta^{94/90}$Zr values calculated from our experiments. Because no arrays that are co-linear with the origin of this plot are defined among experiments sharing any given base mix, the scatter is unlikely to be caused by a melt chemistry dependence (*e.g.*, variable M, ASI or A/NK) of the fractionation factor. Our high T experiments exhibit the largest $\Delta^{94/90}$Zr scatter at any given T and define a steep array with a slope indicative of non-equilibrium fractionation.

Non-equilibrium trace element and isotope partitioning is expected to develop in solids growing from a magma when the distribution coefficient ($K_D = [i]_{solid}/[i]_{liquid}$) of a species of interest [*i*] diverges from unity, with the magnitude of the effects increasing proportionally to the ratio of phase boundary migration velocity over the diffusivity of the species in question (Albarede and Bottinga, 1972; Watson and Müller, 2009; Watkins *et al.*, 2017). Although analytical expressions to quantify this process in radial coordinates exist (*e.g.*, Eq. 11 of Watson and Müller, 2009), these are not applicable to the case of zircon growth as the conditions for this process are outside the bounds over which the Watson and Müller (2009) relationships are accurate (*i.e.* these apply for trace species where $K_D < \approx 0.5$). Thus, at present, the magnitude of Zr isotope fractionation during diffusion limited growth of magmatic zircon is better approached numerically.

To test for a possible kinetic control on isotope fractionation in our experiments, we used the numerical approach of Bindeman and Melnik (2022) to calculate an expected $\Delta^{94/90}$Zr *vs.* $1/T^2$ relation for zircon nucleating at 1400 °C and using model parameters close to those of our experimental conditions (see Supplementary Information). Because β factors (an empirical parameter describing the efficiency of diffusive isotope fractionation; Richter *et al.*, 1999) for Zr in melt have not yet been determined, we do not attempt to reproduce our experiments quantitatively. However, it can be clearly seen from Figure 2 that the slope of kinetic isotope fractionation in $\Delta^{94/90}$Zr *vs.* $1/T^2$ space closely resembles the trend defined by our high T experiments, and is also similar to the slope of the Guo *et al.* (2020) model defined using natural zircon nucleated at lower temperatures. Thus, we interpret these steep arrays that do not intersect the origin of a $\Delta^{94/90}$Zr *vs.* $1/T^2$ plot as reflecting a combination of equilibrium and kinetic isotope fractionation effects, resulting in a compounded, larger fractionation than what can be imparted by vibrational equilibrium processes alone. Nevertheless, because β factors for Zr remain unknown, quantitative deconvolution of kinetic and equilibrium fractionation contributions to natural and experimental $\Delta^{94/90}$Zr data is not yet possible.

Given the above observations, we consider the experiments performed at high T (low *f*) inadequate for quantifying an equilibrium fractionation coefficient, and instead argue that the results from our highest *f* experiments ($n = 4$ where $f \geq 0.9$)) yield the $\Delta^{94/90}$Zr that *most closely approach* the magnitude of the equilibrium fractionation factor. Indeed, isotope effects recorded by a solid growing in a kinetically dominated system where $K_D >> 1$ are significant at low *f* (*e.g.*, Fig. 12 of Watson and Müller, 2009), whereas the impact of kinetic fractionation on the *cumulative* solid composition must, by mass balance, approach zero as *f* tends to unity. Results from experiments where $f \geq 0.9$ yield a mean $\Delta^{94/90}$Zr of −0.045 ‰. Although these experiments can potentially also be affected to some small degree by kinetic isotope effects, they all tightly cluster between the $\Delta^{94/90}$Zr models of Chen *et al.* (2020) and Méheut *et al.* (2021) (Fig. 2), supporting the accuracy of these first principles calculations. While our results cannot distinguish which of these two theoretical models is more accurate, we note that the absolute difference in $\Delta^{94/90}$Zr at magmatic T between these studies is exceedingly small. As such, our results experimentally confirm their predictions, and reinforce the notion that large fractionations observed in natural zircon cannot be the result of equilibrium fractionation processes.

Overall, our results are in excellent agreement with the direction of isotopic fractionation estimated from *ab initio* studies and, for our lowest T experiments ($f \geq 0.9$), also its magnitude. Our results thus confirm that the expected effects of equilibrium isotope fractionation during magmatic zircon crystallisation are

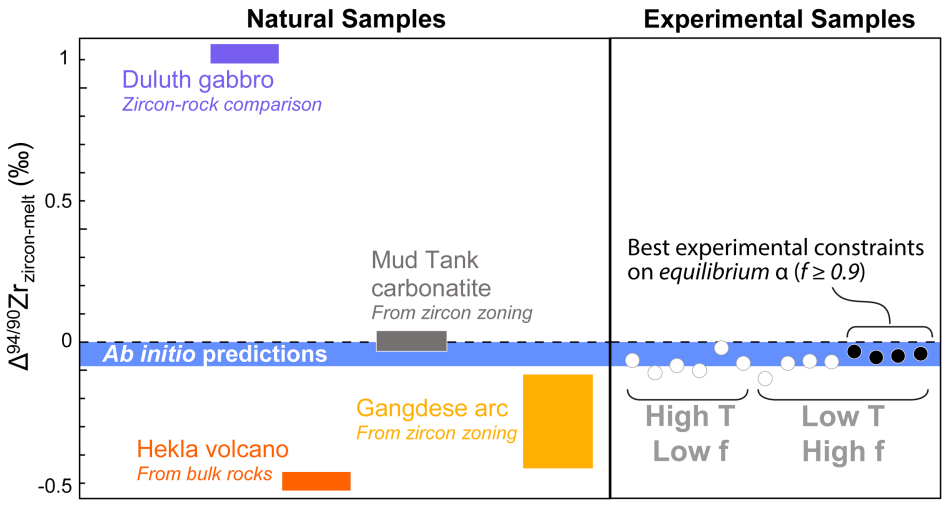

Figure 3 Summary of zircon-melt fractionation factors from *ab initio* calculations at ≥700 °C (Chen *et al.*, 2020; Méheut *et al.*, 2021), natural samples (Ibañez-Mejia and Tissot, 2019; Inglis *et al.*, 2019; Guo *et al.*, 2020; Tompkins *et al.*, 2020), and experimental samples (this study).

exceedingly small, demonstrating that the observed range of natural variability cannot be explained by this mechanism (Fig. 3). Instead, and as argued by Chen *et al.* (2020), Méheut *et al.* (2021), and Tissot and Ibañez-Mejia (2021), we conclude that non-equilibrium effects are needed to explain, and must be the dominant driver of, the large Zr isotope variations observed in natural systems.

Conclusions and Implications

This study demonstrates that: 1) at equilibrium, zircon is isotopically light compared to its co-existing silicic melt; 2) the magnitude of equilibrium Zr isotope fractionation between zircon and melt at magmatic temperatures is extremely small ($\Delta^{94/90}Zr \approx -0.045$ ‰), as predicted by *ab initio* calculations; and 3) the large $\delta^{94/90}Zr$ variations observed in natural igneous systems to date are not the result of equilibrium fractionation during zircon crystallisation. Our results reinforce the notion that kinetic isotope effects play a central, if not the dominant, role in fractionating Zr isotopes in high temperature environments. Thus, additional experimental constraints that quantify the magnitude of kinetic separation of Zr isotopes in solids and liquids (*e.g.*, Watkins *et al.*, 2017) are needed before the fractionations observed in natural systems can be fully understood and quantified.

Acknowledgements

This project was supported by NSF Graduate Research Fellowship award DGE-1746060, an MSA Student Research Grant, and a GSA Student Research Grant (to HGDT), as well as NSF-EAR grants 2131632 and 2143168 (to MIM), 1824002 (to FLHT), 1650033 (to DT), and SNSF Ambizione grant PZ00P2_173988 (to EB). FLHT acknowledges additional support from NSF grant MGG-2054892, a Packard Fellowship, a research award from the Heritage Medical Research Institute, and startup funds from Caltech. The authors thank editor Anat Shahar, James Van Orman, and an anonymous reviewer, for constructive reviews that improved the clarity of this article.

Editor: Anat Shahar

Additional Information

Supplementary Information accompanies this letter at https://www.geochemicalperspectivesletters.org/article2310.

Cite this letter as: Tompkins, H.G.D, Ibañez-Mejia, M., Tissot, F.L.H, Bloch, E., Wang, Y., Trail, D. (2023) Zircon growth experiments reveal limited equilibrium Zr isotope fractionation in magmas. *Geochem. Persp. Let.* 25, 25–29. https://doi.org/10.7185/geochemlet.2310

References

Albarede, F. and Bottinga, Y. (1972) Kinetic disequilibrium in trace element partitioning between phenocrysts and host lava. *Geochimica Cosmochimica Acta* 36, 141–156. https://doi.org/10.1016/0016-7037(72)90003-8

Bindeman, I.N. and Melnik, O.E. (2022) The rises and falls of zirconium isotopes during zircon crystallisation. *Geochemical Perspectives Letters* 24, 17–21. https://doi.org/10.7185/geochemlet.2241

Boehnke, P., Watson, E.B., Trail, D., Harrison, T.M., and Schmitt, A.K. (2013) Zircon saturation re-revisited. *Chemical Geology* 351, 324–334. https://doi.org/10.1016/j.chemgeo.2013.05.028

Chen, X., Wang, W., Zhang, Z., Nie, N.X., and Dauphas, N. (2020) Evidence from *Ab Initio* and Transport Modeling for Diffusion-Driven Zirconium Isotopic Fractionation in Igneous Rocks. *ACS Earth and Space Chemistry* 4, 1572–1595. https://doi.org/10.1021/acsearthspacechem.0c00146

Cherniak, D.J., Hanchar, J.M., and Watson, E.B. (1997) Diffusion of tetravalent cations in zircon. *Contributions to Mineralogy and Petrology* 127, 383–390. https://doi.org/10.1007/s004100050287

Criss, R.E. (1999) *Principles of Stable Isotope Distribution*. Oxford Univ Press, New York. https://doi.org/10.1093/oso/9780195117752.001.0001

Guo, J.L. Wang, Z., Zhang, W., Moynier, F., Cui, D., Hu, Z., Ducea, M. (2020) Significant Zr isotope variations in single zircon grains recording magma evolution history. *Proceedings of the National Academy of Sciences* 117, 21125–21131. https://doi.org/10.1073/pnas.2002053117

Ibañez-Mejia, M., and Tissot, F.L.H. (2019) Extreme Zr stable isotope fractionation during magmatic fractional crystallization. *Science Advances* 5, eaax8648. https://doi.org/10.1126/sciadv.aax8648

Inglis, E.C., Moynier, F., Creech, J., Deng, Z., Day, J.M.D., Teng, F.Z., Bizzarro, M., Jackson, M., and Savage, P. (2019) Isotopic fractionation of zirconium during magmatic differentiation and the stable isotope composition of the silicate Earth. *Geochimica Cosmochimica Acta* 250, 311–323. https://doi.org/10.1016/j.gca.2019.02.010

Méheut, M., Ibañez-Mejia, M., and Tissot, F.L.H. (2021) Drivers of zirconium isotope fractionation in Zr-bearing phases and melts: The roles of vibrational, nuclear field shift and diffusive effects. *Geochimica Cosmochimica Acta* 292, 217–234. https://doi.org/10.1016/j.gca.2020.09.028

Richter, F.M., Liang, Y., and Davis, A.M. (1999) Isotope fractionation by diffusion in molten oxides. *Geochimica Cosmochimica Acta* 63, 2853–2861. https://doi.org/10.1016/S0016-7037(99)00164-7

Schauble, E.A., Méheut, M., and Hill, P.S. (2009) Combining Metal Stable Isotope Fractionation Theory with Experiments. *Elements* 5, 369–374. https://doi.org/10.2113/gselements.5.6.369

Tissot, F.L.H., and Ibañez-Mejia, M. (2021) Unlocking the single-crystal record of heavy stable isotopes. *Elements* 17 (6), 389–394. https://doi.org/10.2138/gselements.17.6.389

Tompkins, H.G.D., Zieman, L.J., Ibañez-Mejia, M., and Tissot, F.L.H. (2020) Zirconium stable isotope analysis of zircon by MC-ICP-MS: Methods and application to evaluating intra-crystalline zonation in a zircon megacryst. *Journal of Analytical Atomic Spectrometry* 35, 1167–1186. https://doi.org/10.1039/C9JA00315K

Wang, Y., and Trail, D. (2019) Aluminum partitioning between zircon and haplogranitic melts: The influence of temperature and melt composition. *Chemical Geology* 511, 71–80. https://doi.org/10.1016/j.chemgeo.2019.02.016

Watkins, J.M., DePaolo, D.J., and Watson, E.B. (2017) Kinetic fractionation of non-traditional stable isotopes by diffusion and crystal growth reactions. *Reviews in Mineralogy and Geochemistry* 82, 85–125. https://doi.org/10.2138/rmg.2017.82.4

Watson, E.B., and Müller, T. (2009) Non-equilibrium isotopic and elemental fractionation during diffusion-controlled crystal growth under static and dynamic conditions. *Chemical Geology* 267, 111–124. https://doi.org/10.1016/j.chemgeo.2008.10.036

Young, E.D., Manning, C.E., Schauble, E.A., Shahar, A., Macris, C.A., Lazar, C., and Jordan, M. (2015) High-temperature equilibrium isotope fractionation of non-traditional stable isotopes: Experiments, theory, and applications. *Chemical Geology 395*, 176–195. https://doi.org/10.1016/j.chemgeo.2014.12.013

Zhang, W., Wang, Z., Moynier, F., Inglis, E., Tian, S., Li, M., Liu, Y., and Hu, Z. (2019) Determination of Zr isotopic ratios in zircons using laser-Ablation multiple-collector inductively coupled-plasma mass-spectrometry. *Journal of Analytical Atomic Spectrometry 34*, 1800–1809. https://doi.org/10.1039/C9JA00192A